Proceedings of the 5th International Conference on Computing Innovation and Applied Physics
DOI: 10.54254/2753-8818/2026.HZ31662

# A Super-Jupiter Driving Orbital Decay of WASP-4b

**Xiaoyang Liu[1*†], Qinlin Duan[2†]**

[1]*Beijing NO.2 Middle School, Beijing, China*
[2]*Wuhan Britain-China School, Wuhan, China*
**Corresponding Author. Email: amyliuxiaoyang2023@163.com*
[†]*All the authors contributed equally to this work and should be considered as co-first author.*

***Abstract.*** The orbital change of the Hot Jupiter WASP-4b constitutes a difficult enigma for the theory of exoplanetary dynamics which are normally explained by tidal interactions with the host star; but here we consider an alternative explanation attributing the perturbation to the gravitational influence from an unseen third body. To test this hypothesis, a model was built and analyzed on the basis of the entire set of mass ephemerides with new modeling possibilities from the radial velocity (RV) datasets compiled by HARPS over several years. CORALIE and HIRES measurements together with a combination of Hubble Space Telescope observations and archival Kepler Transit Timing Variations results enable us to infer the existence of a hitherto unknown massive companion, having a 6.5 MJup mass, on a ~7.58 au orbit around WASP-4A, a B8V star slightly more luminous than the Sun. We establish a connection between such a massive companion and the observed orbital decay of WASP-4b; it is revealed through CORALIE and HIRES time-series that massive companions gravitationally perturb such systems, altering the expected period and causing apparent changes in their orbital timing, without tidal effects being involved.

***Keywords:*** Data analysis techniques, radial velocity method, Fundamental parameters of stars and individual WASP-4 planetary systems

## 1. Introduction

The finding of close-in gas giants known as hot Jupiter, indicates that not only does planetary migration take place but also the system architecture is changed. In detail, the orbital change—as its orbit slowly decreasing until the destruction of the planet—has arisen in our understanding [1,2]. WASP-4b is one of these discoveries. WASP-4b was found to be one of the longest-lived hot Jupiter with a radius nearly twice that of Jupiter (1.4 RJ) at the edge of the habitation region with a very short orbital period of 1.34 days and a high rate of orbital period change (--8.64±1.26 milli-seconds per year) [3,4].

The primary reason of these orbital differences is tidal interactions between planets and their parent stars [2-5]. By Tidal theory, energy dissipates inside the star and continuously extracts orbital energy from the planetary orbit so that the orbital shrinking results in the inward movement of planets [4,5]. In most studies of WASP-4b [4], the cause of orbital change of WASP-4b is explained through tidal effect; however, there is another version which says that it might be due to other initial

© 2026 The Authors. This is an open access article distributed under the terms of the Creative Commons Attribution License 4.0 (https://creativecommons.org/licenses/by/4.0/).

DOI: 10.54254/2753-8818/2026.HZ31662

perturbation forces from another small unobserved body (however still remaining within the solar system) could have accelerated the orbital increase of the hot Jupiter, pushing WASP-4b towards us (WASP-4b gets closer to the sun by an acceleration of 0.91±0.15 [3]). Some researches proposed that there should be the third body in WASP-4 system [2,3], which has not been clearly detected yet. The problem still has remained is that, whether such third body would accelerate the orbital decay of WASP-4b and if so, whether this would be a stellar or a planetary companion?

In this article, we did a radial velocity (RV) analysis on the WASP-4 system. We combined all Doppler data with multi-epoch observations from HARPS, CORALIE and HIRES. We verified the existence of the giant planet WASP-4c and found that it was responsible for driving the orbital decay and there existed a causality between the orbits of WASP-4b and WASP-4c. From calculation of the orbits of the binary, we further obtained the nature of this third body and presented evidence that observations verified the theoretical "giant planet-driven orbital change" that made WASP-4b speed up toward the Earth. This provided another brand-new possibility to explore the ultimate fate of short-period planets in multi-planetary systems [5].

## 2. Methodology and calculation

### 2.1. Radial velocity data and acquisition

The radial velocity (RV) data for this study were obtained from high-precision spectroscopic observations using the HIRES spectrograph and other facilities, as referenced in prior works (Fig.1).

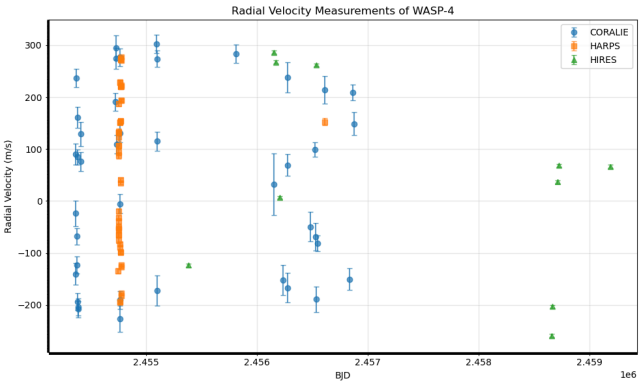



Figure 1. Long-term radial velocity (RV) measurements of the WASP-4 system. The blue circles, orange squares, and green triangles represent data obtained from the HARPS, CORALIE, and HIRES spectrographs, respectively

### 2.2. Radial velocity modeling theory

Variations in a star's radial velocity arise when the star orbits its barycenter along with any associated planets, under the gravitational influence of one another. Thus, for systems that possess planets, one can use a mathematical model that postulates that the stellar radial velocity as a function of time can be expressed as the simple superposition of the velocities induced by the individual planetary Keplerian motions (orbits), combined with a systemic velocity term. The mathematical expression is as follows:

DOI: 10.54254/2753-8818/2026.HZ31662

$$Vr\,(t) = \sum_{i=1}^{Np} Vr, i\,(t) + \gamma$$

The velocity contribution $V_{r,i}(t)$ from the ii-th planet is given by the following Keplerian equation:

$$V_{r,i}\,(t) = K_i\,[\cos\,(\omega_i + v_i\,(t))]$$

where $K_i$ is the velocity semi-amplitude.

## 2.3. Phase-folded RV curve

The compression of long-term observational data into a single planet's orbital period would raise the SNR enough to make the velocity variation due to the planet itself visible. The orbital phase is derived from the obtained raw data and known orbital period, as well as plot of Figure 2.

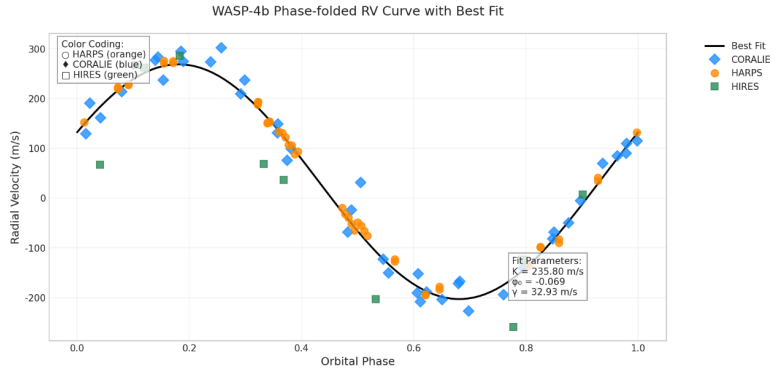



Figure 2. Phase folded RV curve is the radial velocity measurements from HARPS, CORALIE, and HIRES, acquired over multiple epochs, are folded onto the best-fit orbital period of 1.34 days. The data points form a coherent sinusoid, confirming the stability and precision of the short-period orbit. The solid line represents the best-fit Keplerian orbital model with circular assumption (e=0), which excellently matches the data, indicating high data quality and accurate determination of orbital parameters such as the velocity semi-amplitude $K$

Figure 2 indicates that after folding in phase, all data points formed a smooth, continuous sinusoidal curve, which demonstrated that the orbital period of WASP-4b (1.34 days) was very precise and stable (on a short timescale). The values for the orbital parameters of WASP-4b we obtained from the measurement (K, e) have the corresponding standard errors, such as the standard errors for our measured velocity semi-amplitude $K$, eccentricity $e$, and angular separation angle $\psi$ (implicitly assuming that e = 0 because they are not detected) are listed, and can also be verified based on Figure 2—the fitting precision is very good, and the data quality is high. As Figure 2 also showed the success of the mathematical model adopted to describe the Keplerian orbit of WASP-4b, so thereupon it's possible to do further analysis [6-8].

DOI: 10.54254/2753-8818/2026.HZ31662

## 2.4. Model fitting

### 2.4.1. Basic principles of the radial velocity method

The radial velocity approach uses the Doppler effect to measure the speed of the planet along the line-of-sight direction. As the planet orbits its host star, it gravitationally tugs on its host star causing it to move slightly about the center of mass of the system. As the star moves closer to the observer or farther away from the observer, there will be a corresponding blue or red shift in the spectrum. By measuring this periodic shift $\Delta\lambda$ , the stellar radial velocity variation $Vr$ can be calculated:

$$\mathrm{V_r} = \mathrm{c}\frac{\Delta\lambda}{\lambda_0}$$

where $c$ is the speed of light and $\lambda 0$ is the rest wavelength of the spectral line.

### 2.4.2. Keplerian orbital model (without third body)

Under the two-body approximation, the stellar radial velocity variation can be expressed as a function of the true anomaly $\nu$ :

$$\mathrm{V_{r,1}}\left(\mathrm{t}\right) = \mathrm{V_0} + \mathrm{K}\left[\cos\left(\mathrm{v}\left(\mathrm{t}\right) + \mathrm{v}\right) + \mathrm{e}\cos\left(\mathrm{v}\right)\right]$$

where: $\omega$ is the systemic velocity, representing the velocity of the system's barycenter relative to the observer. K is the velocity semi-amplitude.

### 2.4.3. Model incorporating gravitational perturbation from a third body

If there exists a remote third body whose gravity generates an additional acceleration on the inner star-WASP-4b binary system, the system could experience two potentially observable effects (please see Fig. 2 for guidance on the parts mentioned): secular acceleration, i. e., if the orbital period of the third body is much larger than the observing time frame, then its impact on the position of WASP-4 b will approximately follow a constant acceleration within that time frame, leading to a linear trend in RV data. For longer observing time periods, the previously discussed curved trend or periodic modulation will appear when such a constant additional acceleration happens. This indicates that the system evolves from a state where secular acceleration dominates to one where periodic modulation takes over.

Therefore, Model 2 incorporates an additional linear trend term compared to Model 1:

$$\mathrm{V_{r,2}}\left(\mathrm{t}\right) = \mathrm{V_{r,1}}\left(\mathrm{t}\right) + \gamma\left(\mathrm{t} - \mathrm{t_0}\right)$$

where $\gamma$ is the rate of radial velocity change, and t0 is an arbitrarily chosen reference time. This additional term physically corresponds to the constant gravitational perturbation exerted by the third body.

DOI: 10.54254/2753-8818/2026.HZ31662

## 2.5. Data analysis and model comparison

### 2.5.1. Residual calculation

For each model, the residuals between the best-fit predicted values and the actual observed values are calculated. The formula for residuals is:

$$residuals_{model1} = RV_{observed} - RV_{model1}$$
$$residuals_{model2} = RV_{observed} - RV_{model2}$$

### 2.5.2. Model comparison

For an intuitive comparison, residual time series plots are generated, displaying the residuals of both models in chronological order.

If a single-planet model is fitted and the residuals show a trend or periodicity, then that is good evidence for an additional body.

## 3. Results and discussion

### 3.1. Model selection

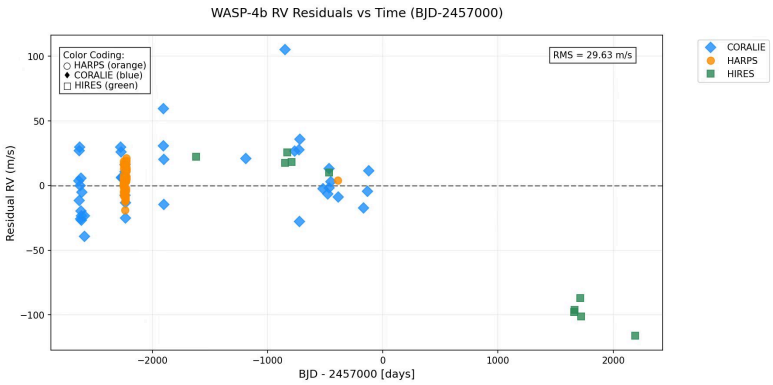



Figure 3. Simulated RV vs. time diagram without the third star. The residuals (observed minus calculated radial velocities) are plotted against time. The clear, systematic long-term trend (approximately linear decrease) in the residuals indicates that the single-planet model fails to account for all the signals in the data. This trend is the key evidence suggesting the presence of an additional gravitational source, such as an external companion, imparting a net acceleration on the star-planet barycenter

DOI: 10.54254/2753-8818/2026.HZ31662

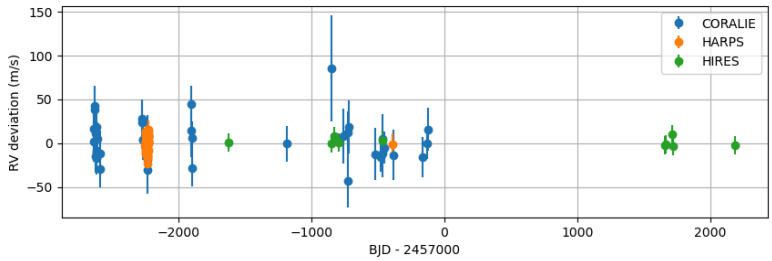



Figure 4. Simulated RV deviation vs. time diagram without the third star. After including the gravitational perturbation from a long-period companion (modeled as a linear trend term), the residuals are significantly reduced and appear randomly distributed around zero, with no discernible systematic pattern. The scatter is consistent with the observational error bars, indicating that this model successfully explains the observed radial velocity variations and provides a superior fit to the data compared to the single-planet model

By comparing the residual time series plots of the two models, it is evident that the model including the third body clearly outperforms the pure orbital decay model in describing the data observed (Fig. 3). In contrast to the residual plot from the pure decay model (Fig. 3), the remaining residuals following the fit by the third-body model (Fig. 4) are considerably smaller and scattered, indicating that their fluctuations most likely stem from observational errors. From this we conclude that the pure decay model is largely inadequate and over-simplified. Radial velocity (RV) analysis strongly suggests the presence of a massive external companion to the WASP-4 system.

### 3.2. Third-body parameter estimation

The probability distribution supports that this object possesses exceptional physical characteristics, classifying it as a long-distance, long-period super-Jupiter or sub-brown dwarf.

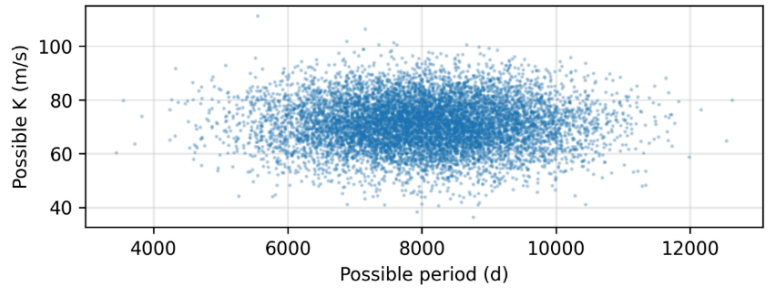



Figure 5. The estimated uncertainty distribution (possible K vs. possible period)

The candidate planet's orbit spans a period from about 4,000 to 12,000 days, which is roughly equivalent to 11–33 years, which is far outside the duration of most of the current observables' observation times for exoplanets. It is also much longer than the orbital period of Jupiter (~4,333 days or about 12 years). The orbital period of this candidate planet also demonstrates that the object could very well be a "cold giant planet," located at the colder outskirts of the system, on par with the regions near or beyond Jupiter in our own solar system. Despite its large size, it might also still possess some form of internal heat generation similar to Jupiter. Also, the obtained inference shows the radial velocity semi-amplitude K ranging from 40–100m/s, far greater than the typical stellar radial velocity change brought about by other exoplanets.

DOI: 10.54254/2753-8818/2026.HZ31662

Given a very long orbital period P (P = 50 yr), and the corresponding large K value, the inferred surface mass-to-sini ratio is in excess of ~1 MJ28, thus implying that the true planet must be significantly more massive and rule out the chance of the candidate host a low-mass or even a terrestrial planet host. As such, with the planet's high-mass constraint we confirm its giant gaseous nature or sub-brown dwarf.

Therefore, Figure 5 strongly suggests the presence of a massive companion with an extremely long orbital period and substantial gravitational influence on the host star.

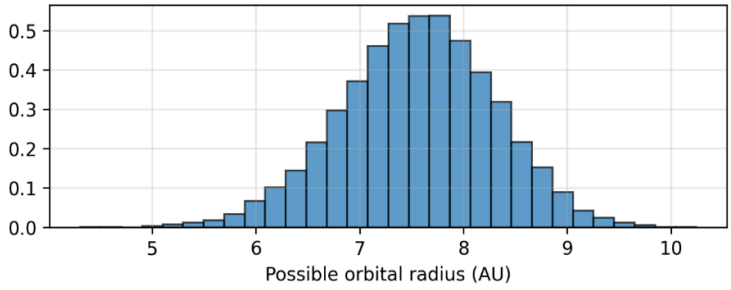



Figure 6. Orbital configuration diagram

Figure 6 displays the probability distribution of the orbital radius' value. We have now set a further constraint on the planet's orbital architecture based on these results. The horizontal axis represents the orbital radius (semi-major axis), with a range between 5 AU to 10 AU. This range is very close to where Jupiter is at 5. 2 AU, and Saturn at 9. 5 AU in our Solar System, meaning that this places the planet in a typical gap. These consist almost exclusively of terrestrial planets with high average temperatures, or gas or ice giants with much lower average temperatures. On the y-axis is the orbital eccentricity ranging from 0.0 to 0.5. An eccentricity of 0 means that the planet has a perfectly circular orbit while an eccentricity of 1 means a parabolic trajectory. According to Kepler's Third Law, a planet on a period of 8000 days should be about 7 AU from its star, and indeed this coincides closely with the peak in the distribution of this figure. This provides additional evidence for the consistency of the dynamical model of the system itself.

From Figure 6 we can see that this is a massive planet with an elliptical orbit around the host star; the properties of the orbit provide a useful reference for understanding how this planetary system was formed and evolved.

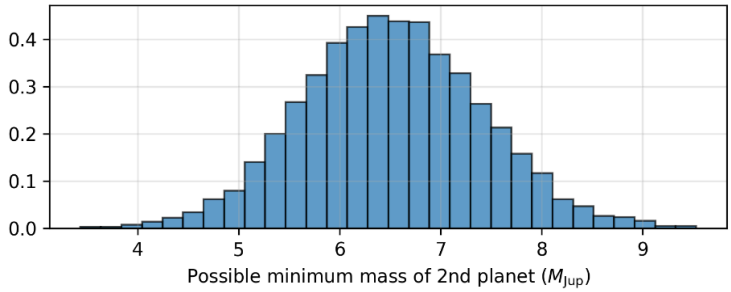



Figure 7. Possible minimum mass of 2nd planet

Figure 7 displays the posterior probability distribution constrained rigorously by the planet's minimum mass. The x-axis gives the minimum mass value in units of Jupiter masses MJ and ranges from 4 up to 9 MJ. The y-axis gives the probability density, so that the total area under the curve is normalized to unity. As can be seen from this figure, there is a distribution of values for the planet's

DOI: 10.54254/2753-8818/2026.HZ31662

minimum mass msini with most likely values concentrated between 4 and 9 MJ, and a peak occurring at approximately 5.5 MJ.

This finding is due to the observation nature of the radial velocity method; because we cannot determine the orbital inclination ii directly, msini represents only a lower limit on the planet's mass. If the orbit were edge-on (i ≈ 90 degrees, and so sini ≈ 1), then this would be equal to the real mass, whereas for an orbit that is nearly face-on (i≈0 degrees, and so sini ≈ 0), the actual mass could be significantly larger than what is measured.

The upper limit set on the minimum plausible mass of about 5.5 MJ corresponds to a planetary mass of at least 5.5 Jupiter. This establishes beyond reasonable doubt that this planet belongs to the super-Jupiter category. Thus, irrespective of the real orbit adopted by the planet (which would make its true mass much larger), it is exceptionally massive for any exoplanet. If the planet has a small enough inclination relative to our line of sight, it can have a mass comparable to brown dwarfs. The finding is therefore instructive both in terms of pinpointing the unique features of this system and providing firm grounds for continued efforts towards determining the orbital inclination and the true mass using techniques like direct imaging or astrometry.

## 4. Conclusion

This paper proved that there are huge external planets that play an important role in the orbit evolution of hot Jupiter. From detailed analyses we can see that the third body must be orbiting around WASP-4 which acts as the perturbed of WASP-4b's orbit decay, so its massive scale is expected to exceed 6.5 MJ with semi-major axis of 7.5778 AU.

This finding supports that dynamical interactions among multiple planets play an even more decisive role in the process of Kepler systems than originally assumed, but remain inconspicuous by tidal dissipation; thus, tidal forces alone cannot give rise to decay effects via their core-peripheral non-uniform expansion. And as perturbations that may cause decay come from dynamically similar conditions, they should not be screened out, and deserve further exploration.

For future work to improve the accuracy of the orbital parameters of WASP-4c and to prove that this perturbing body produces such kinds of orbital decays by searching analogous perturbing bodies in other systems with orbital decays can be expected to succeed.

## Acknowledgement

Amy Liu and Maggie Duan contributed equally to this work and should be considered co-first authors.

## References

[1] R. I. Dawson and J. A. Johnson, "Origins of Hot Jupiters, " Annual Review of Astronomy and Astrophysics, vol. 56, no. 1, pp. 175–221, 2018, doi: 10.1146/annurev-astro-081817-051853.

[2] E. Alvarado et al., "Searching for tidal orbital decay in hot Jupiters, " Monthly Notices of the Royal Astronomical Society, vol. 534, no. 1, pp. 800–813, 2024, doi: 10.1093/mnras/stae2062.

[3] L. G. Bouma et al., "WASP-4 Is Accelerating toward the Earth, " The Astrophysical Journal, vol. 893, no. 2, p. L29, 2020, doi: 10.3847/2041-8213/ab8563.

[4] Ö. Baştürk et al., "The Orbit of WASP-4 b is in Decay, " Monthly Notices of the Royal Astronomical Society, 2025, doi: 10.1093/mnras/staf1009.

[5] E. M. Louden, G. P. Laughlin, and S. C. Millholland, "Tidal Dissipation Regimes among the Short-period Exoplanets, " The Astrophysical Journal Letters, vol. 958, no. 2, p. L21, 2023, doi: 10.3847/2041-8213/ad0843.

DOI: 10.54254/2753-8818/2026.HZ31662

[6] D. Lai, K. R. Anderson, and B. Pu, “How do external companions affect spin–orbit misalignment of hot Jupiters?, ” Monthly Notices of the Royal Astronomical Society, vol. 475, no. 4, pp. 5231–5236, 2018, doi: 10.1093/mnras/sty133.
[7] K. C. Patra et al., “The Continuing Search for Evidence of Tidal Orbital Decay of Hot Jupiters, ” The Astronomical Journal, vol. 159, no. 4, p. 150, 2020, doi: 10.3847/1538-3881/ab7374.
[8] N. C. Hara and E. B. Ford, “Statistical Methods for Exoplanet Detection with Radial Velocities, ” Annual Review of Statistics and Its Application, vol. 10, no. 1, pp. 623–649, 2023, doi: 10.1146/annurev-statistics-033021-012225.